

Preparation and characterization of nanosized zirconium (hydrous) oxide particles

Luis A. Pérez-Maqueda^{a)} and Egon Matijević^{b)}

Center for Advanced Materials Processing, Clarkson University, Potsdam, New York 13699-5814

(Received 12 December 1996; accepted 5 August 1997)

A method for the preparation of nanosized zirconium (hydrous) oxide particles of narrow size distribution is described. The procedure yields stable dispersions at low temperatures and short reaction times in the absence of surfactants, using inorganic zirconium salts. Crystal structure, particle size distribution, electrokinetic properties, stability, and thermal behavior of the prepared particles were investigated. Colloidal dispersions were treated with ultrasound to study their effect on the crystal structure of the calcined samples.

I. INTRODUCTION

Colloidal nanosized zirconium oxide is of interest for its applications as ceramic material,¹ solid electrolyte,² corrosion product in nuclear reactors,³ and for the fundamental understanding of the formation of colloidal metal oxides.

Common methods for the preparation of fine particles of zirconia include hydrolysis of Zr-alkoxide solutions,^{4,5} of aerosol droplets of Zr-alkoxide⁶ or ZrO(NO₃)₂ solutions,⁷ or of zirconium salt solutions by urea,^{8,9} hydrothermal precipitation from gels,¹⁰⁻¹³ aqueous precipitation-phase extraction route,¹⁴ and the microwave heating of zirconium salt solutions.¹⁵

This study describes the preparation of uniform nanosized zirconium (hydrous) oxide particles by precipitation in homogeneous solutions of ZrCl₄ in the presence of triethanolamine. The samples are characterized in terms of particle size distribution, structure, as well as their changes on calcination and ultrasonic treatment. The stability of the dispersions in the presence of different electrolytes was evaluated.

II. EXPERIMENTAL

A. Materials

Reagent grade zirconium tetrachloride (Aldrich), triethanolamine (TEA, Aldrich), sodium nitrate (J. T. Baker Analyzed), sodium sulfate (J. T. Baker Analyzed), and tungstosilicic acid hydrate (Fluka) were used without further purification. Solutions were prepared with doubly distilled water, and all solutions were filtered through 0.2 μm pore size Nuclepore membranes to remove any possible particulate contaminants. Zirconium chloride

solutions were not kept for more than two days to avoid the precipitation of hydroxides. The solutions were checked with a laser for clarity before being used.

B. Particle preparation

The precipitation procedure consisted of the following steps: (i) Solutions of zirconium chloride and triethanolamine (TEA) were preheated independently to the same desired temperature. (ii) The heated zirconium chloride solution was poured into the TEA solution in air, followed by aging at the same reaction temperature for 1 h with continuous agitation. (iii) The resulting suspension was quenched to room temperature by immersing it into an ice water bath. (iv) The particles were separated by centrifugation at 30,000 rpm, the supernatant solutions were then discarded, and the particles were washed four times with doubly distilled water. (v) The solid was dried at 60 °C overnight.

To study the influence of the ultrasonic energy on the samples, some of the final dispersions were treated intermittently for 6 h with an ultrasonic probe, dipped vertically into the system placed in a cylindrical cooled container. During the sonication cycle ultrasound was on for 1 and off for 2 min.

C. Particle characterization

Zirconium (hydrous) oxide particles were examined by scanning (SEM) and transmission (TEM) electron microscopy. For TEM, carbon coated 200 mesh copper grids were placed into a centrifuge tube containing a very dilute dispersion of the particles, and spun at 10,000 rpm for 20 min. The grids with deposited samples were dried on a filter paper.

The particle size distribution was estimated from dynamic light scattering (Brookhaven Instrument Corp.) with an argon-ion laser of 514.6 nm wavelength at a 90° angle. The data were analyzed using the CONTIN

^{a)}On leave from Instituto de Ciencia de Materiales de Sevilla, Centro Mixto C.S.I.C., Universidad de Sevilla, Apdo. 1115, 41080 Sevilla, Spain.

^{b)}Author to whom correspondence should be addressed.

program.¹⁶ In order to avoid coagulation during the dynamic light-scattering measurements, diluted samples were acidified to pH 4 with HCl, which yielded a very stable dispersion.

The electrophoretic mobilities were measured as a function of the pH with a Delsa 440 (Coulter Electronics) instrument. The ionic strength was maintained constant by dispersing the particles in a 0.01 mol dm^{-3} NaCl

solution, and the pH of the dispersion was adjusted with HCl and NaOH as needed.

The crystalline structures of the solids were assayed by x-ray diffraction and IR spectroscopy. The dimensions of the coherently diffracting domains (crystallite size) of tetragonal zirconia were determined from the full-width of the half maximum of the peak (111) using the Scherrer equation.¹⁷

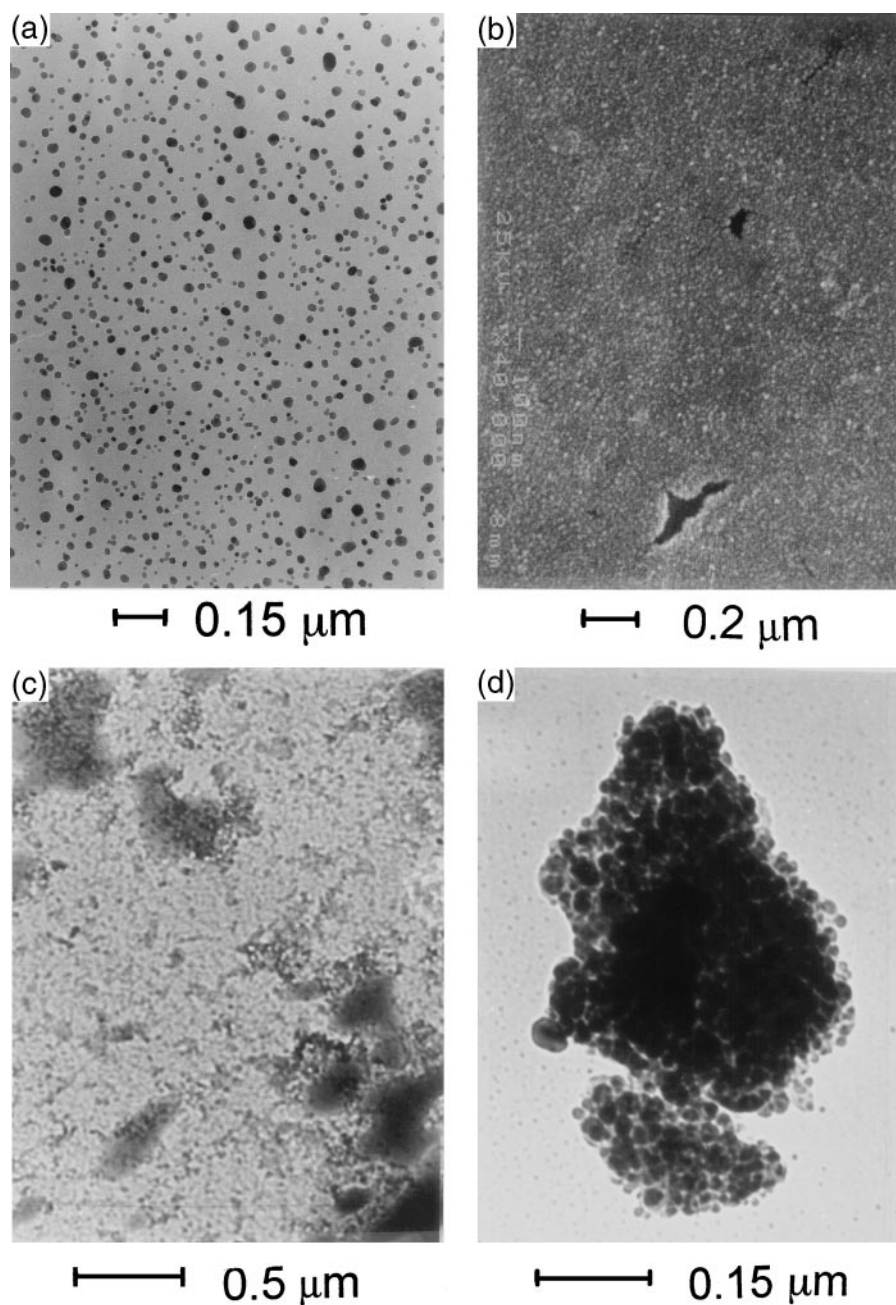


FIG. 1. Transmission (TEM) (a) and scanning (SEM) (b) electron micrographs of the zirconium (hydrrous) oxide particles obtained by aging at $95 \text{ }^\circ\text{C}$ for 1 h an aqueous 0.01 mol dm^{-3} zirconium chloride solution containing 0.2 mol dm^{-3} triethanolamine (TEA) at $\text{pH} = 8$. (c) TEM of the sample obtained under the same conditions as above but at room temperature. (d) TEM for the zirconium (hydrrous) oxide sample illustrated in (a) after calcination at $400 \text{ }^\circ\text{C}$ for 2 h.

Thermogravimetric (TG) and differential scanning calorimetry (DSC) analyses of the samples were carried out in the flow of air, at heating rates of 20 and 40 °C min⁻¹, respectively.

The coagulation rate in the dispersion containing different concentrations of electrolytes was followed with a universal light scattering instrument (Phoenix Precision Instrument Company) using an incident unpolarized light beam of 546 nm wavelength. The intensity of scattered light measured at 90° was divided by the intensity of the incident beam and plotted as a function of time.

III. RESULTS AND DISCUSSION

Zirconium (hydrous) oxide dispersions of narrow size distribution were obtained when solutions, 0.01 mol dm⁻³ in ZrCl₄ and 0.2–0.8 mol dm⁻³ in TEA (molar ratio [TEA]/[ZrCl₄] in the range 20 to 80) were aged for different intervals of time (1–2 h) and over a range of temperatures (25–95 °C). The reaction yield was dependent on the [TEA]/[ZrCl₄]; at the smallest ratio ([TEA]/[ZrCl₄] = 20) the yield was 24%, calculated for ZrO₂, and for [TEA]/[ZrCl₄] = 80 it was 63%.

Smaller concentrations of the reactants, up to ten times less, but with the same [TEA]/[ZrCl₄] ratios as above, produced similar particles. As examples, dispersions shown in Figs. 1(a)–1(c) were produced in solutions having [TEA]/[ZrCl₄] = 20 under conditions mentioned in the legends of these figures. Higher concentrations of the reactants than those reported before, produced gelatinous or aggregated materials.

Figure 2 shows the change in the particle size distribution (established by light scattering) at 25, 55, and 95 °C in a system containing 0.01 mol dm⁻³ ZrCl₄ and 0.2 mol dm⁻³ TEA (i.e., [TEA]/[ZrCl₄] = 20) aged for 1 h. The aqueous dispersion obtained at 25 °C was then heated at 95 °C to check for any possible changes. In all these experiments, the ZrCl₄ solution was mixed with preheated solutions of TEA. The samples obtained at 25 °C and 55 °C had the same particle size distribution [Figs. 2(a) and 2(c)], as the one generated at 25 °C and then heated at 95 °C [Fig. 2(b)]. The mean hydrodynamic diameter of the last three samples was 27 ± 16 nm, which is somewhat smaller than when the system was aged at 95 °C [38 ± 18 nm, Fig. 2(d)]. The average size of the same particles, as determined from electron microscopy [Fig. 1(a)], was 33 ± 9 nm. A small peak in the particle size distributions of all samples at higher particle size is probably due to minor aggregation.

The importance of the mixing order of the solutions during precipitation has been recognized before,^{18,19} because it may alter the nucleation and growth stages. One experiment was performed to study the influence of reversing the addition order of the solutions on the final product. The preheated solution of TEA was poured into

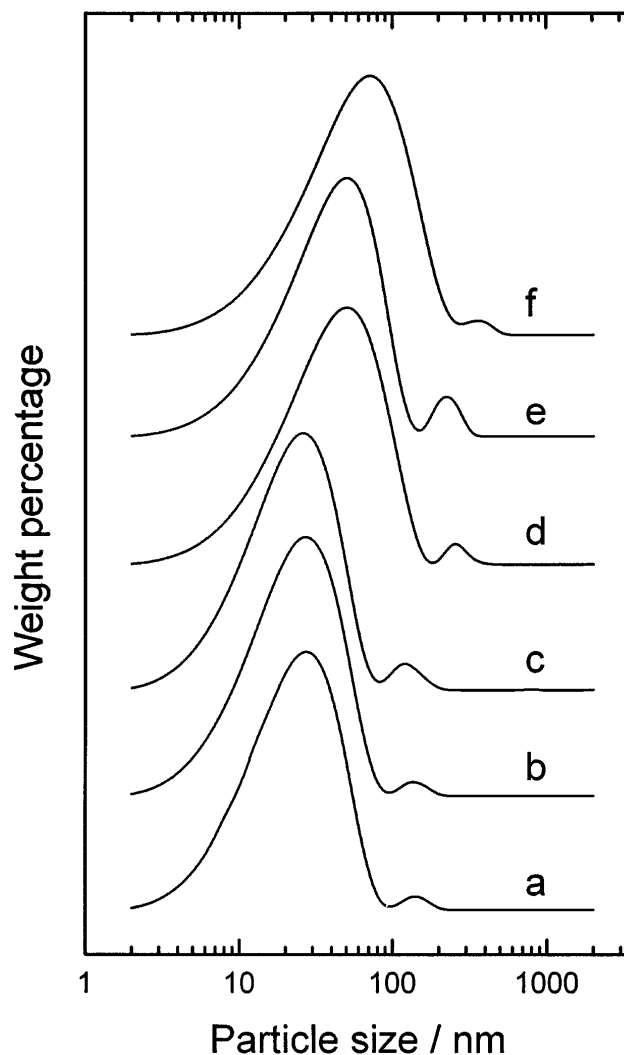


FIG. 2. Particle size distributions determined by dynamic light scattering for the samples obtained by aging for 1 h an aqueous 0.01 mol dm⁻³ zirconium chloride solution containing 0.2 mol dm⁻³ TEA at pH = 8, then washed several times with water and redispersed in aqueous solutions of pH = 4. The aging temperatures were (a) 25 °C, (b) 25 °C for 1 h and then heated at 95 °C for an additional hour, (c) 55 °C, (d) 95 °C, (e) 95 °C and stored for 120 days, and (f) 95 °C but changing the mixing order.

the solution of ZrCl₄, but no influence was observed in the particle size distribution [Fig. 2(f)].

Colloid dispersions prepared at optimum conditions remained stable after washing, if acidified to pH 4 (using HCl) without the use of surfactants. Figure 2(e) confirms that the particle size distribution of the sample obtained at 95 °C [Fig. 2(d)] does not change after 120 days of storage.

The IR spectrum (Fig. 3) of the particles shown in Fig. 1(a) after drying shows a strong absorption at 470 cm⁻¹ due to the Zr–O vibration. The intense bands at 3385 and 1630 cm⁻¹ are characteristic of a highly hydrated compound. Bands at 1085, 1370, and 2880 cm⁻¹

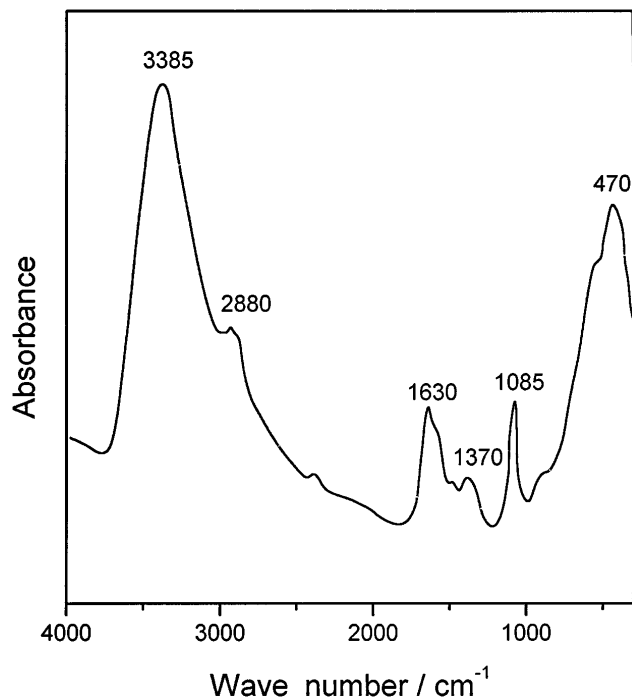


FIG. 3. IR spectrum of the particles shown in Fig. 1(a) after washing 4 times with water and drying at 60 °C overnight.

can be attributed to the inclusion of a very small amount of TEA that remains incorporated even after washings. TEA does not play a role only in the precipitation of zirconium (hydrated) oxide by increasing the pH of the reaction, but may also stabilize the precipitated particles.

The plot of electrokinetic mobilities as a function of the pH for zirconium (hydrated) oxide particles [illustrated in Fig. 1(a)] yields an isoelectric point (i.e.p.) at pH \sim 8.2 [Fig. 4(a)]. It is difficult to compare this value with other literature data, since the i.e.p. points reported for zirconia and hydrous zirconia varied from 3 to 11.4, depending on the preparation method, impurities, hydration degree, etc.^{3,9,10,13,14,20–26} The observed i.e.p. at pH 8.2 for zirconia may be attributed to its highly hydrated nature.²⁷

Electrolytic coagulation experiments of the sample illustrated in Fig. 1(a) were conducted at pH 4, at which zirconium (hydrated) oxide particles carried a positive charge [Fig. 4(a)] using KNO_3 , Na_2SO_4 , and $\text{H}_4\text{SiW}_{12}\text{O}_{40}$ as coagulants; consequently, NO_3^- , SO_4^{2-} , and $\text{SiW}_{12}\text{O}_{40}^{4-}$ acted as counterions. Figures 5, 6, and 7 show plots of the relative intensity measured at 90° as a function of time for different concentrations of these anions. A decrease in I_{90}/I_0 indicated that the dispersion was destabilized and settled, leaving a supernatant solution of low turbidity. The critical coagulation concentration (ccc) was taken as the lowest value of the added counterion, which caused a sharp drop in the scattering intensity with time. The so

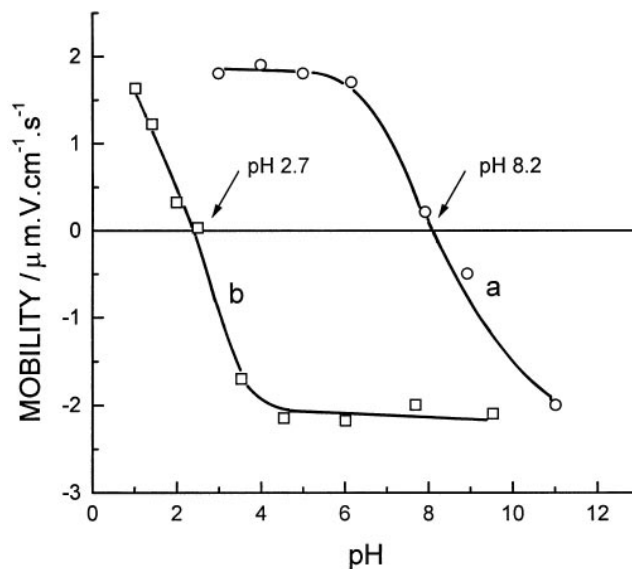


FIG. 4. Electrophoretic mobility as a function of the pH of (a) the zirconium (hydrated) oxide sample illustrated in Fig. 1(a) and (b) same sample in the presence of $1 \times 10^{-4} \text{ mol dm}^{-3} \text{ H}_4\text{SiW}_{12}\text{O}_{40}$.

obtained ccc for NO_3^- was $3.5 \times 10^{-3} \text{ mol dm}^{-3}$, for SO_4^{2-} $7 \times 10^{-5} \text{ mol dm}^{-3}$ and for $\text{SiW}_{12}\text{O}_{40}^{4-}$ $2 \times 10^{-4} \text{ mol dm}^{-3}$. The first two values are as expected according to the well-known Schulze–Hardy rule, while the ccc for the tungstosilicate ion is rather high. The same anion destabilizes hydrophobic colloids, such as silver halides, at a considerably lower concentration ($\sim 10^{-7} \text{ mol dm}^{-3}$).²⁸ Different coagulation ability of this anion in the case of zirconium (hydrated) oxide dispersions may be due to the complex formation between

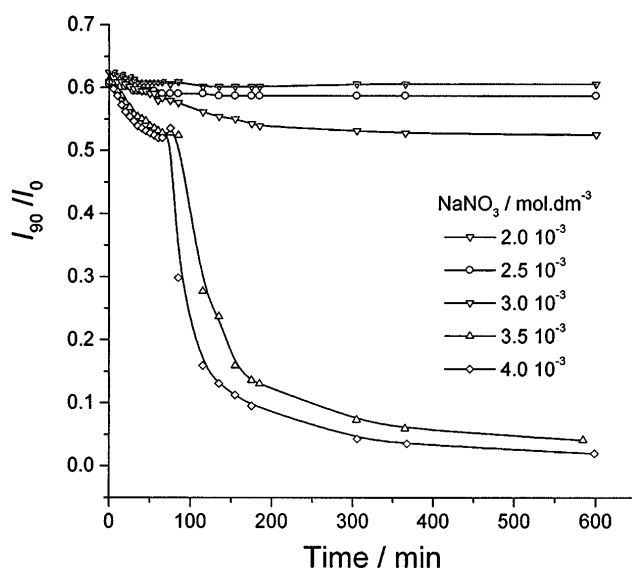


FIG. 5. Relative scattering intensities (I_{90}/I_0) as a function of time for different concentrations of added NaNO_3 , for 1.5% aqueous dispersion at pH = 4 of the sample illustrated in Fig. 1(a).

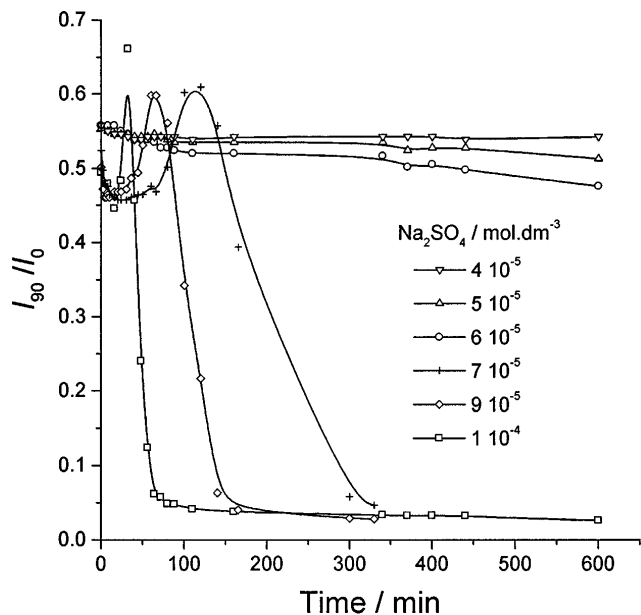


FIG. 6. The same plots as in Fig. 4 for added Na_2SO_4 .

the surface zirconium site and the heteropoly anion. In order to ascertain experimentally if such interaction takes place, electrokinetic measurements with the zirconium (hydrous) oxide dispersions were performed in the presence of $\text{SiW}_{12}\text{O}_{40}^{4-}$ ($1 \times 10^{-4} \text{ mol dm}^{-3}$), and a shift in the i.e.p. from $\text{pH} = 8.2$ to $\text{pH} = 2.7$ [Fig. 4(b)] was observed. The charge of the zirconium (hydrous) oxide particles, coagulated at $\text{pH} = 4$ in the presence of $5 \times 10^{-4} \text{ mol dm}^{-3}$ of $\text{H}_4\text{SiW}_{12}\text{O}_{40}$, was established to be negative by electrophoretic mobility. Thus, the coagulation of this dispersion by the tungstosilicate ion is caused by the neutralization of the surface charge

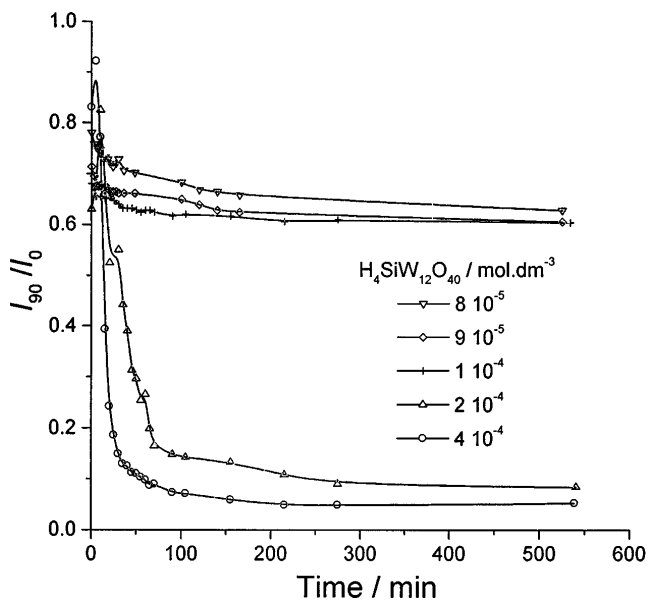


FIG. 7. The same plots as in Fig. 4 for added $\text{H}_4\text{SiW}_{12}\text{O}_{40}$.

at the low pH. The floc is then rendered negatively charged by the adsorption of excess $\text{SiW}_{12}\text{O}_{40}^{4-}$.

In a separate study, it was shown that mixing solutions of ZrCl_4 and $\text{H}_4\text{SiW}_{12}\text{O}_{40}$ produced precipitates, which under certain conditions consisted of uniform spherical particles.²⁹

The x-ray diffraction (XRD) pattern of the original zirconium hydrous oxide sample is characteristic of amorphous solids [Fig. 8(a)], regardless of the experimental conditions.

The thermogravimetric analysis of the sample of Fig. 1(a) after drying overnight at 60°C showed a weight loss of 10.3% on heating to 200°C , 21.5% to 300°C , 29.1% to 460°C , and 32.4% to 900°C . The differential scanning calorimetry (DSC) (Fig. 9) indicates an endothermic process at $\sim 160^\circ\text{C}$, which can be attributed to the dehydration of the sample, and an exothermic process at $\sim 355^\circ\text{C}$, due to the crystallization of the amorphous particles (so-called glow phenomenon³⁰). This crystallization temperature is lower than those reported in the literature,^{8,30-33} which vary between 390°C and 470°C . The reason for the differences may be in the particle size: the finely divided powder should be more reactive than those of larger particles. The exothermic effect is broader than reported in the literature^{30,33} for the crystallization process; there is possibly a contribution of the decomposition of the TEA impurities that overlaps with the crystallization effect.

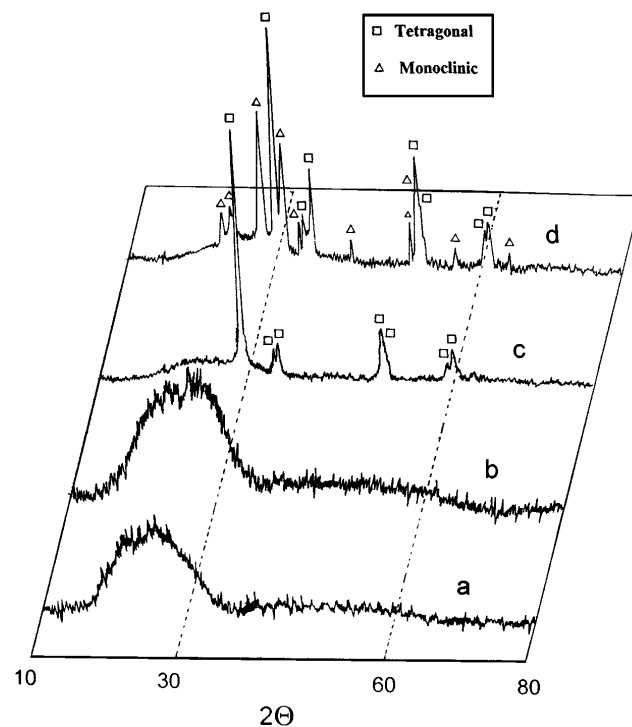


FIG. 8. XRD diagrams for the zirconium (hydrous) oxide samples: (a) original [Fig. 1(a)] and heated for 2 h at (b) 300°C , (c) 400°C , and (d) 950°C .

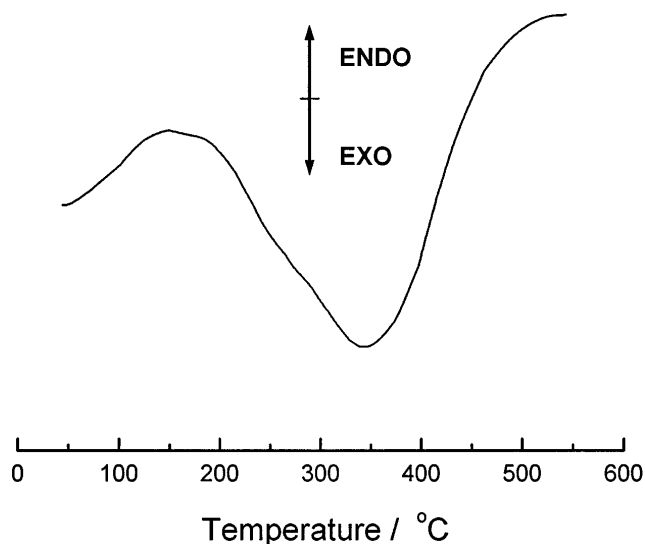


FIG. 9. Differential scanning calorimetry (DSC) plot in air flow at $40\text{ }^{\circ}\text{C min}^{-1}$ for the zirconium (hydrus) oxide sample illustrated in Fig. 1(a).

Figures 8(b)–8(d) show the XRD spectra of the same sample calcined for 2 h at 300, 400, and 950 °C. At 300 °C the solid is still amorphous, as can be expected from the DSC results. When heated to 400 °C, which is above the crystallization temperature, the pattern is characteristic of the tetragonal phase, in agreement with the IR spectrum of the same sample heated at 400 °C [Fig. 10(a)]. The absorption bands at 590, 485, and 350 cm^{-1} indicate the tetragonal structure,

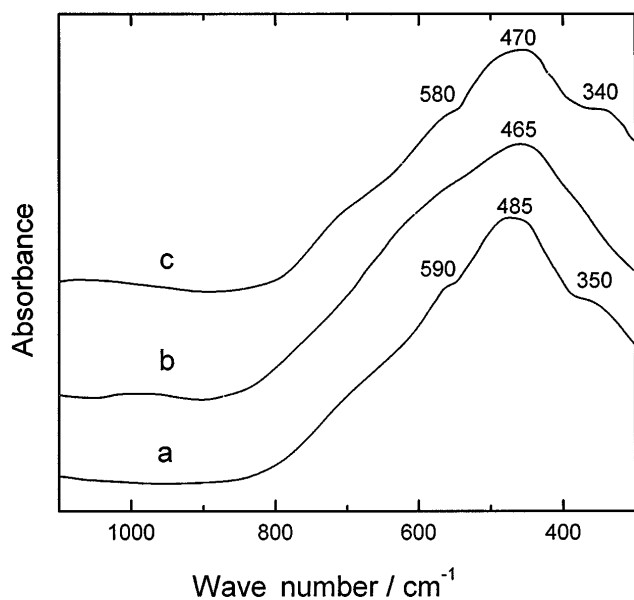


FIG. 10. IR spectra in the range $1100\text{--}300\text{ cm}^{-1}$ of the zirconium (hydrus) oxide sample shown in Fig. 1(a): (a) calcinated at 400 °C for 2 h, (b) first ultrasonically treated and then calcinated at 500 °C for 2 h, and (c) first ultrasonically treated and then calcinated at 550 °C for 7 h.

as described elsewhere.³⁴ The sample heated to 950 °C is constituted of a mixture of tetragonal and monoclinic phases [Fig. 8(d)].

The full-width of the half maximum of the (111) diffraction peak (the most intensive) for the sample calcined at 400 °C yielded a crystallite size of 36 nm. This finding shows that particles are aggregates of nanosized subunits [Fig. 1(d)], consisting of single crystallites (coherent diffraction domains), the size of which is the same as that of the hydrous zirconia [Fig. 1(a)]; consequently, during the calcination every original amorphous particle is transformed into a single crystallite.

Dispersion of particles illustrated in Fig. 1(a), subjected to ultrasonic energy, underwent aggregation and settling. The XRD of the sample so treated at room temperature indicated particles to be amorphous [Fig. 11(a)], but on heating the powder at 400 or 500 °C for 2 h, the XRD pattern became characteristic of the cubic structure [Fig. 11(b)], in agreement with the IR data [Fig. 10(b)]. This result differs from the behavior of the original sample (without ultrasonication), which changed into the tetragonal form at the same calcination temperature. The cubic particles eventually recrystallize into tetragonal, if kept sufficiently long $>550\text{ }^{\circ}\text{C}$ [Figs. 10(c) and 11(c)].

The agglomeration of particles after ultrasonic treatment was reported previously.^{35,36} The smaller the particles, the stronger is the influence of the vibrational motion produced by sonication. Suslick³⁵ explained this effect for metallic powders by the cavitation effect. The latter produces hot spot conditions with high local

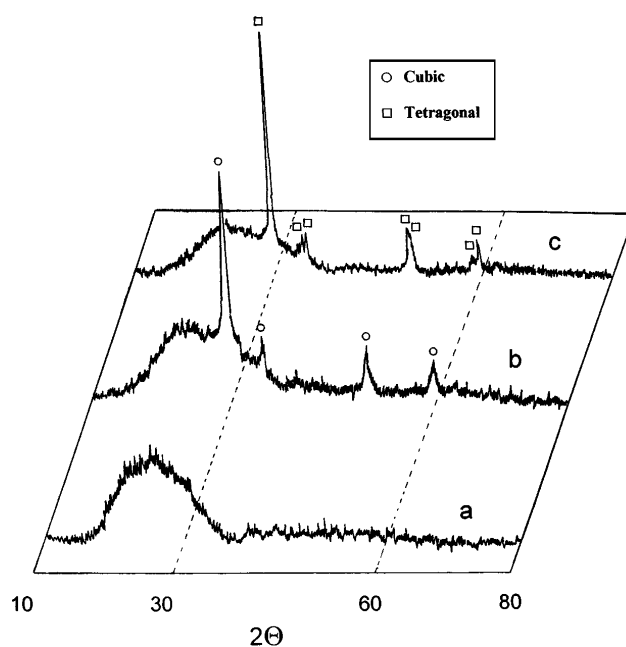


FIG. 11. XRD patterns of the zirconium (hydrus) oxide sample after ultrasonication: (a) without further treatment, (b) calcinated at 500 °C for 2 h, and (c) calcinated at 550 °C for 7 h.

temperatures and pressures of short duration. Sonication was also used as a method to change crystal properties of organic compounds³⁷; it specifically induced the transformation of tetragonal to monoclinic zirconia.³⁸ It is noteworthy that the amorphous particles produced in this study subjected to ultrasounds show different behavior than so untreated solids. Ultrasonic energy produced structural transformations in the zirconium (hydrous) oxide by stabilizing the cubic phase at room temperature even when the sample was calcined at temperatures as high as 500 °C for 1 h.

ACKNOWLEDGMENTS

This work was supported by NSF grant 9423163. A grant to L. A. P-M. from the Dirección General de Investigación Científica y Técnica (Ministry of Education and Culture from Spain) is gratefully acknowledged. The authors want to express their appreciation to Dr. Yie-Shein Her for useful discussions at the early stages of this research.

REFERENCES

1. D. J. Clough, *Ceram. Eng. Sci. Proc.* **6**, 1244 (1995).
2. P. Hafenmüller and W. Van Gool, *Solid Electrolytes* (Academic Press, New York, 1978).
3. M. A. Blesa, A. J. G. Maroto, S. I. Passaggio, N. E. Figliolia, and G. Rigotti, *J. Mater. Sci.* **20**, 4601 (1985).
4. L. Lerot, F. Legrand, and P. Bruycker, *J. Mater. Sci.* **26**, 2353 (1991).
5. B. E. Yoldas, *J. Mater. Sci.* **21**, 1080 (1986).
6. M. Ocaña, V. Fornes, and C. J. Serna, *Ceram. Int.* **18**, 99 (1992).
7. T. Yoshioka, K. Dosaka, T. Sato, A. Okuwaki, S. Tanno, and T. Miura, *J. Mater. Sci. Lett.* **11**, 51 (1992).
8. H. Yue-Xiang and G. Cun-Ji, *Powder Technol.* **72**, 101 (1992).
9. B. Aiken, W. P. Hsu, and E. Matijević, *J. Mater. Sci.* **25**, 1886 (1990).
10. S. Ardizzone, M. G. Cattania, P. Lazzari, and P. Lugo, *Colloids Surf.* **90**, 45 (1994).
11. S. Komarneni, R. Roy, E. Breval, M. Ollinen, and Y. Suwa, *Adv. Ceram. Mater.* **1**, 87 (1986).
12. P. E. D. Morgan, *J. Am. Ceram. Soc.* **69**, C204 (1984).
13. E. Tani, M. Yoshimura, and S. Sōmiya, *J. Am. Ceram. Soc.* **66**, 11 (1983).
14. A. W. L. Dudeny, M. Abdel-Ghani, G. H. Kelsall, A. J. Monhemius, and L. Zhang, *Powder Technol.* **65**, 207 (1991).
15. Y. T. Moon, D. K. Kim, and C. H. Kim, *J. Am. Ceram. Soc.* **78**, 1103 (1995).
16. S. W. Provencher, *Comput. Phys. Commun.* **27**, 215 (1982).
17. P. Scherrer, *Gött. Nachr.* **2**, 98 (1918).
18. M. D. Rasmussen, G. W. Jordan, M. Akinc. O. Hunter, Jr., and M. F. Berard, *Ceram. Int.* **9**, 59 (1983).
19. D. M. Avila and E. N. S. Muccillo, *Thermochim. Acta* **256**, 391 (1995).
20. P. H. Tewari and W. Lee, *J. Colloid Interface Sci.* **52**, 77 (1975).
21. S. Ardizzone, G. Bassi, and G. Liborio, *Colloids Surf.* **51**, 207 (1990).
22. G. Ajay and E. Matijević, *J. Colloid. Interface Sci.* **126**, 243 (1988).
23. A. E. Regazzoni, M. A. Blesa, and A. J. G. Maroto, *J. Colloid Interface Sci.* **91**, 560 (1983).
24. G. W. Smith and T. Salmon, *Can. Metall. Q.* **5**, 93 (1966).
25. G. B. Amphlett, L. A. McDonald, and M. J. Redman, *J. Inorg. Nucl. Chem.* **6**, 263 (1958).
26. M. Schultz, St. Grimm, and Buckhardt, *Solid State Ionics* **63–65**, 18 (1993).
27. G. Parks, *Chem. Rev.* **65**, 177 (1965).
28. E. Matijević and M. Kerker, *J. Phys. Chem.* **62**, 62 (1958).
29. A. Koliadima, L. A. Pérez-Maqueda, and E. Matijević, *Langmuir* **13**, 3733 (1997).
30. G. Gimblett, A. A. Rahman, and K. S. W. Sing, *J. Chem. Tech. Biotech.* **30**, 51 (1980).
31. E. Crucean and B. Rand, *Trans. J. Brit. Ceram. Soc.* **78**, 58 (1979).
32. A. Benedetti, G. Fagherazzi, F. Pinna, and S. Polizzi, *J. Mater. Sci.* **25**, 1473 (1990).
33. G. Štefanić, S. Popović, and S. Musić, *Thermochim. Acta* **259**, 225 (1995).
34. C. M. Phillipy and K. S. Mazdiyasn, *J. Am. Ceram. Soc.* **54**, 254 (1971).
35. K. S. Suslick, *MRS Bull.* **74**, 29 (1995).
36. A. Delgado and E. Matijević, *Part. Part. Syst. Charact.* **8**, 128 (1991).
37. R. Srinivasan, I. Z. Shirgaonkar, and A. B. Pandit, *Sep. Sci. Technol.* **30**, 2239 (1995).
38. T. Mitsuhashi, M. Ichihara, and U. Tatsuke, *J. Am. Ceram. Soc.* **57**, 97 (1974).